Res Chem Intermed (2014) 40:2269–2276
DOI 10.1007/s11164-014-1604-y

Cysteine-assisted growth of silver on gold nanorods

Jin-Pei Deng · Jyun-Hao Lin · Cheng-Yung Hsu

Received: 20 January 2014 / Accepted: 15 February 2014 / Published online: 26 March 2014

Abstract Au–Ag core–shell (Au@Ag) nanobars could be synthesized from gold nanorod (NR) seeds with cysteine additives by a two-step process of reaction temperatures. The lateral sides of gold NRs surrounded by surfactant bilayers render cysteine additives binding on both ends of the NRs, and restricted silver deposition to their lateral sides at room temperature. Further, silver deposition can take place at first on the pre-formed silver layers on the lateral sides at higher temperatures and finally resulted in the formation of Au@Ag nanobars in which gold NRs are in the corner positions of the nanobars and their longitudinal axes parallel to the longer sides of the nanobars.

Keywords Gold nanorod · Core–shell nanoparticle · Nanobar

Introduction

Among gold nanoparticles that have been well prepared, gold nanorods (NRs) of one-dimensional nanomaterials have been frequently synthesized and studied in the last decade [1–4]. Because gold nanoparticles exhibit surface plasmon resonance (SPR) bands, gold NRs with controlled aspect ratios (length/width) could have the two characteristic SPR bands (transversal and longitudinal modes) in the visible and near-infrared region [5]. Gold NRs can also be used as both templates and seeds to undergo morphological modification by secondary growths in further reactions [6]. Most of these changes in morphology have the strong influence on the wavelengths and intensities of the SPR bands [7]. For example, gold NR-seeded growths of gold nanoparticles, such as octahedron and cube, have been reported in previous literature [6–8]. It is evident that the wavelengths and numbers of their SPR bands

J.-P. Deng (✉) · J.-H. Lin · C.-Y. Hsu
Department of Chemistry, Tamkang University, New Taipei City 251, Taiwan
e-mail: jpdeng@mail.tku.edu.tw

are quite different from original gold NRs, and strongly related to their geometrical shapes. On the other hand, many researchers have adopted epitaxial growth of silver atoms on the surface of gold NRs [9–11]; the nano-structures of these resulting gold–silver core–shell nanoparticles (Au@Ag NPs) with sharp or slightly truncated corns are useful as the substrate for desorption of the analytes in surface-enhanced Raman scattering (SERS). It has been reported that SERS properties of silver nanocubes are size-dependent [12]. Moreover, silver has a better enhanced factor than that of gold in the detection sensitivity of SERS.

Gold NRs have usually been prepared by wet chemical methods in the aqueous micellar solutions of cetyltrimethylammonium bromide (CTAB) [1, 2]. After centrifugation, as-prepared gold NRs were purified and then used as seeds in the coating reaction of silver. The coating was usually achieved by the reduction of silver ions with ascorbic acid (AA) at room and higher temperatures [10, 11, 13]. The morphology of the final Au@Ag NPs strongly depends on the reduction rate which is altered by reaction temperatures. The room and higher temperatures of the reaction condition represent the kinetic and thermodynamic factors, respectively. In this work, we study the influence of the reaction temperature on the synthesis of Au@Ag NPs from gold NRs via the secondary growth. Gold NRs are first covered with the minor portion of silver at room temperature and further coated at 75 °C. On the other hand, cysteine as an additive is added to the reaction solution before the secondary growth [14]. Experimental results indicate that the shape of the resulting Au@Ag NPs strongly depends on a two-step process of reaction temperatures. And the addition of cysteine is essential to the formation of Au@Ag core–shell nanobars in which gold NRs are in the corner positions of the nanobars and their longitudinal axes parallel the longer sides of the nanobars.

Materials and methods

Chemicals and characterization

Sodium borohydride and silver nitrate were obtained from Alfa Aesar and Sigma-Aldrich, respectively. All other reagents were purchased from Acros.

UV/Vis absorption spectra were recorded on a Hitachi U-3900 spectrophotometer. The transmission electron microscopy (TEM) images were obtained on JEOL JEM-2100F microscopes operating at 200 kV.

Synthesis of Au@Ag NPs

In a typical synthesis of Au@Ag NPs, gold NRs as seeds were prepared by a seed-mediated growth method published by Nikoobakht and El-Sayed [2]. First, 5 mL of an aqueous solution of 2.5×10^{-4} M $HAuCl_4$ and 0.1 M CTAB was prepared. Then, 300 μL of an aqueous ice-cold solution of 10 mM $NaBH_4$ was then added to the above solution with stirring at room temperature. After 3 h, the gold particles in the solution were formed and used as seeds for the synthesis of gold NRs. A growth solution was prepared by mixing 5 mL of an aqueous solution of 5×10^{-4} M

$HAuCl_4$ and 0.1 M CTAB with 50 μL of an aqueous solution of 10 mM $AgNO_3$, followed by the addition of AA (32 μL, 0.1 M) and the gold seed solution (10 μL). After 17 h of reaction time, the reaction solution was centrifuged at 8,000 rpm for 20 min. The supernatant was discarded and the concentration was diluted with 1 mL of a solution of 5 mM CTAB. The same procedure of centrifugation and dilution was repeated to give 25 mL of Au NR-containing solution of 10 mM CTAB. Then, 5 mL of the NR-containing solution of 10 mM CTAB was mixed with $AgNO_3$ (5 or 10 μL, 10 mM) at room temperature, subsequently followed by the addition of AA (6.8 or 17.5 μL, 0.1 M) and NaOH (17.5 μL, 1 M). After 1 h of reaction time, the reaction solution was centrifuged at 8,000 rpm for 15 min. The supernatant was discarded and the concentration was diluted with 5 mL of the solution of 10 mM CTAB. Finally, the solution was mixed with $AgNO_3$ (175 or 170 μL, 10 mM) and AA (68 μL, 0.1 M) at 75 °C for 5 h. In the case of the experiments with additives, cysteine (100 μL, 10 mM) was added to the Au NR-containing solution before any silver coating at room temperature.

Results and discussion

First, we demonstrate that Au@Ag nanobars can be prepared from Au NRs at a higher temperature. It has been reported that gold NRs can be employed as the templates in the preparation of Au@Ag nanobars at higher temperatures [10, 11]. Figure 1 is the UV–Vis absorption spectra of Au NR before and after silver coating in the reaction solution. It is apparent that the four SPR bands are clearly discernible (solid line) after heating. They are centered at 348, 400, 446, and 548 nm. The inset of Fig. 1 is the TEM images of the nanoparticles obtained in the reaction. Gold atoms have higher electron densities than those of silver atoms, so these images confirm that gold NRs can be identified in the center of silver nanobars. And the growth of silver on gold NRs resulted in the SPR bands blue shifted in the formation of Au@Ag nanobars. At the same time, the reaction was performed by a two-step process of reaction temperatures: the minor part of silver (about up to 5.6 %) was first coated on Au NRs at room temperature and the remainder of the silver coating was subsequently completed at 75 °C. Figure 2 shows the absorption spectra of gold NRs after silver coating at both room and higher temperatures. When silver ions were first reduced at room temperature, the SPR band of gold NRs was shifted to 665 nm (dashed line). The occurrence of the blue shift indicates that gold NRs were covered with silver. After the complete coating at 75 °C, the fourth band at the longest wavelength in the nanobars at 548 nm disappeared and the other peaks became broader (solid line) in comparison with those in the normal condition (Fig. 1). The TEM image in the inset of Fig. 2 shows that the ordinary nanoparticles formed in the reaction solution have irregular polyhedron shapes and gold NRs can be found inside the outer silver shells. These Au@Ag NPs with a patchwork quilt of grains are polycrystalline as shown in the TEM image.

In addition, cysteine was employed as an additive to modify the surface of gold NRs via the Au–S bonding at room temperature before any silver coating. Subsequently, cysteine-binding Au NRs were coated with silver under the normal

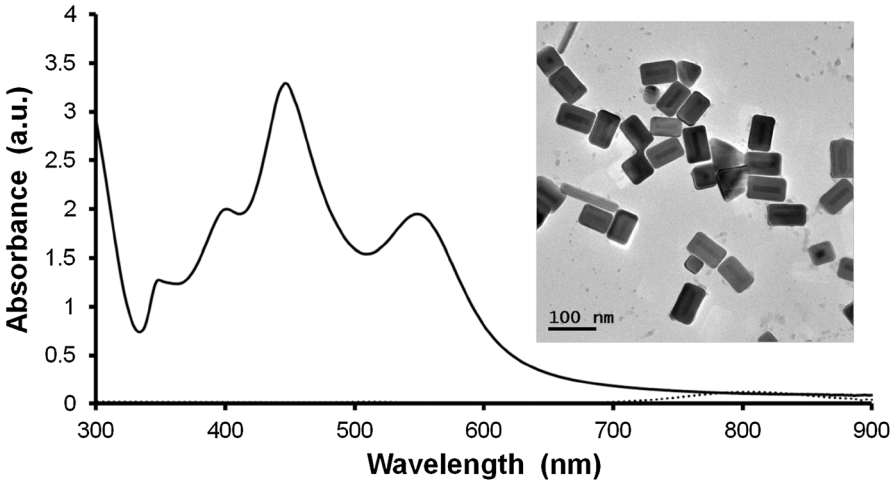

Fig. 1 Absorption spectra of gold NRs before (*dotted line*) and after (*solid line*) the addition of $AgNO_3$ and AA at 75 °C for 5 h. The *inset* shows the TEM images of Au@Ag NPs obtained in the reaction

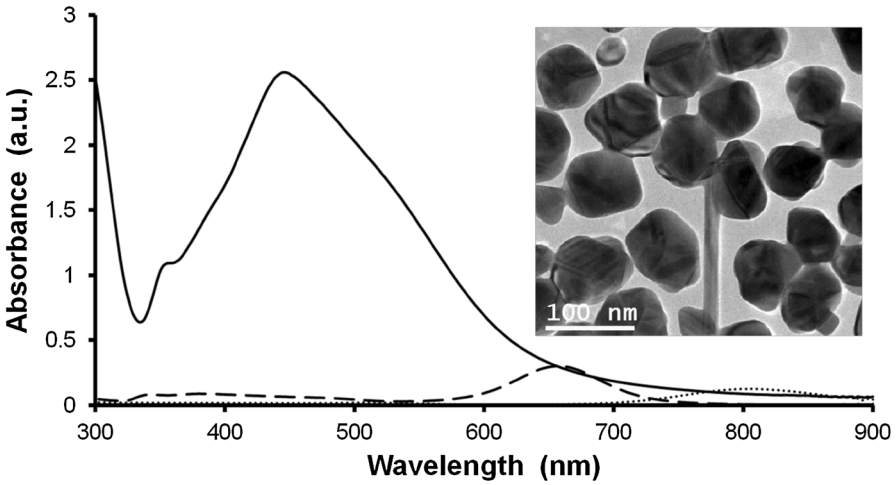

Fig. 2 Absorption spectra of gold NRs before (*dotted line*) and after (*dashed line*) the addition of $AgNO_3$, AA and NaOH at room temperature for 1 h. After centrifugation and purification, the resulting Au@Ag NPs further reacted with $AgNO_3$ and AA at 75 °C for 5 h (*solid line*). The *inset* shows the TEM images of Au@Ag NPs finally obtained in the reaction

reaction condition of 75 °C. It is interesting that the SPR bands of the resulting nanoparticles formed in the reaction solution were similar to those in Fig. 2, but became more shaped. And only a few nanoparticles with regular shapes could be found by TEM. In order to improve the yield, the reaction was also performed by a two-step process of reaction temperatures: cysteine-binding Au NRs were coated with the minor part of silver (about up to 5.6 %) at room temperature and the

remainder of the silver coating was sequentially completed at 75 °C. The absorption spectrum of the as-prepared nanoparticles has a shoulder peak at 384 nm and two peaks at 436 (major) and 352 (minor) nm as shown in Fig. 3. To our surprise, the TEM image in the inset of Fig. 3 shows that some as-prepared nanoparticles have near square cross-sections and the cross-section of several Au NRs is oriented in the corner of the square. When more than 5.6 % of silver is coated at room temperature, most of the as-prepared nanoparticles will finally exhibit irregular morphology under the same reaction condition. Although Au NRs should play the role as seeds to induce the epitaxial growth of silver deposition on them, it is difficult to observe the position of the Au NRs in many nanoparticles. It is possible that the orientation of these nanoparticles on TEM grid did not allow us to find the projection of the Au NRs in the TEM images. Because high-angle annular dark field scanning TEM (HAADF-STEM) can yield the stronger intensity with the increasing atomic number of elements, it was used to discern the Au NR cores in the images of all the nanoparticles with silver shells. The images of the nanoparticles in Fig. 4a, b are obtained in the performance of both the bright-filed and dark-field STEM. The positions of the Au NRs could be easily discernible in Fig. 4a only if their long ends were almost parallel the electron beam. The longitudinal cross-sections of Au NRs seem oriented in the right corner of the squares or bars. However, the positions of the Au NR in every Au@Ag NP becomes prominent in Fig. 4b. Moreover, we can definitely differentiate Au@Ag NPs from Ag NPs in the sample. The latter could be formed by the self-nucleation of Ag NPs in the reaction at the higher temperature. The width and length of Au@Ag nanobars are about 55 and 75 nm, respectively. The aspect ratio of these nanobars is quite a lot smaller than that of the original Au NRs (from 3.8 to 1.4).

Although we can clearly identify the existence of the Au NR core in Au@Ag NPs by HAADF-STEM, the three-dimensional positions of Au NRs are still not well established because their images just belong to the two-dimensional projection by the electron beam in TEM. Therefore, we further performed tilt experiments inside TEM to confirm the three-dimensional orientation of Au NR in the Au@Ag NPs. Figure 5a is the TEM images of the Au@Ag nanobar measured at the different tilted angles. As shown in the left image of Fig. 5a, the cross-section image of Au NR is oriented in the square corner of the Ag outer shell. When the tilting angle is gradually increased to 30° in the x-axial direction, the rod shape of the Au NR can be clearly observed in the right image of Fig. 5a. In particular, the original square is at the same time slowly transformed into a cylindrical shape. These transformations of both Au NR and Ag square shells are simulated in series of the tilting angles as shown in Fig. 5b. Based on the representative tilt images, it can be concluded that the long axis of Au NRs in Au@Ag nanobars parallels the longer sides of the Ag outer shells and is in the corner of the nanobars. The results are also verified by the dark-field image in Fig. 4b.

It is well known that silver epitaxial growth on Au NRs usually results in the formation of Au@Ag NPs with the boat shape in alkaline solutions at room temperature [13]. The rapid deposition of Ag on one of the lateral sides of Au NRs contributes to the asymmetrical shape of the Ag shell. In general, the reduction rate of silver deposition on Au NRs can be predominantly controlled by both the pH of

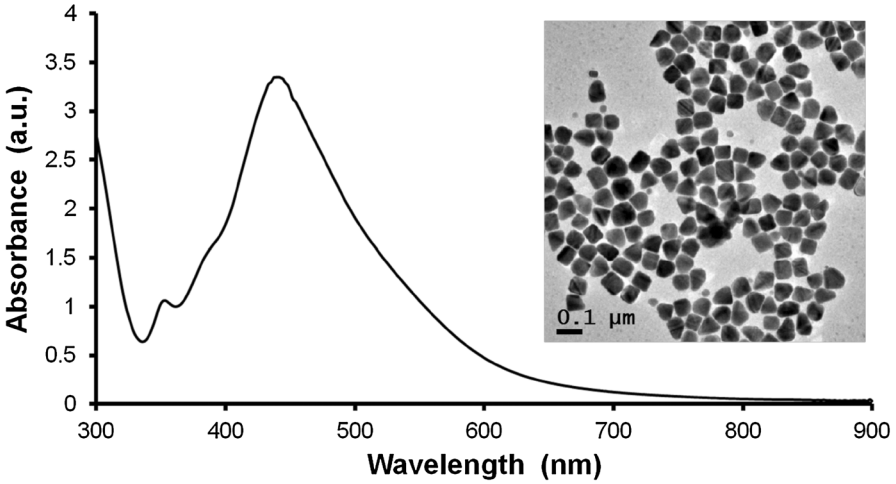

Fig. 3 Absorption spectra of cysteine-binding gold NRs after the addition of $AgNO_3$ and AA at 75 °C for 5 h. The *inset* shows the TEM images of Au@Ag NPs obtained in the reaction

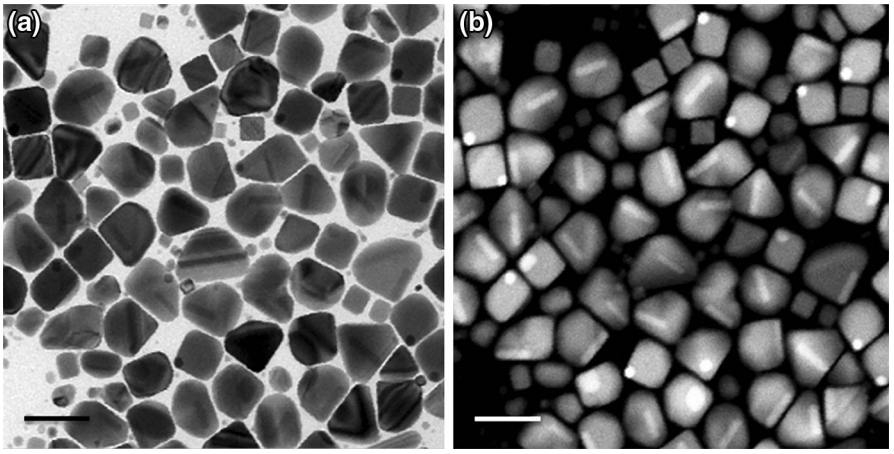

Fig. 4 **a** TEM and **b** the corresponding HAADF-STEM images of Au@Ag NPs obtained in Fig. 3. *Scale bar* 100 nm

the solution and the reaction temperature. Because the reduction rate can be appropriately accelerated by temperatures in an anisotropic epitaxial way, so Au@Ag nanobars can be obtained without the addition of NaOH at a higher temperature [10, 11]. So, it can be expected that the pre-coated Au NR should have the Ag shell with an asymmetrical shape at room temperature. When the Ag pre-coated Au NRs were sequentially used as the seeds, polycrystalline Au@Ag NPs with irregular shapes appeared at the higher temperature as shown in Fig. 2. On the other hand, it is shown that CATB plays an important role in restricting the

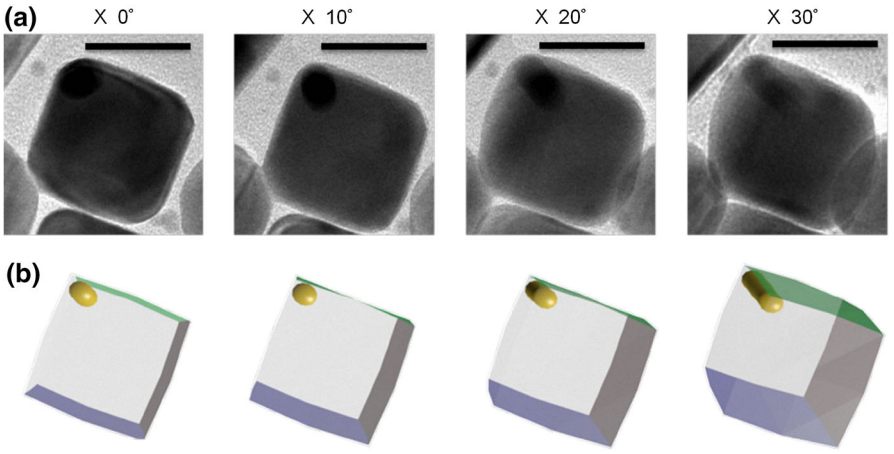

Fig. 5 **a** TEM images of a Au@Ag nanobar at four different tilting angles. **b** The corresponding models are shown for the simulated orientation of each image in **a**. *Scale bar* 40 nm

anisotropic growth of Au NPs in a one-dimensional direction in the preparation of Au NRs. That is, the surfaces of the gold NRs are surrounded by CTAB bilayers in the CTAB reaction. CTAB prefers to bind more strongly to the lateral sides of gold NRs than to their end surface, and thus the chemical modification by cysteine molecules always takes place on both ends of the gold NRs. The characteristic property of the anisotropic binding is useful in the linear assembly of gold NRs by end-to-end arrangements [14–17]. Therefore, the position of the silver coating on cysteine-binding Au NRs is asymmetrically restricted to the lateral sides at room temperature because the two ends modified by cysteine inhibited the epitaxial growth of silver [18]. It is reasonable that the subsequent growth of silver also concentrated on the pre-formed silver layers in the lateral sides of Au NRs by a two-step process of reaction temperatures. In particular, Au@Ag nanobars are enclosed by six {1 0 0} facets in the reported literature [11, 19]. It is possible that silver deposition on cysteine-binding Au NRs occurs at first on some {1 0 0} facets of Au NRs at room temperature and this then gradually leads to the increasing growth on these Ag pre-coated {1 0 0} facets at the higher temperature, finally resulting in the formation of Au@Ag nanobars with six {1 0 0} facets.

Conclusions

We have demonstrated that Au@Ag nanobars can be successfully synthesized from gold NR seeds with cysteine additives by a two-step process of reaction temperatures. Cysteine additives prefer binding on the both ends of gold NRs and subsequently restrict the asymmetrical silver coating to the lateral sides of the Au NRs at room temperature. Further, silver deposition concentrates on the pre-formed silver layers in the lateral sides of Au NRs at higher temperatures and finally results

in the formation of Au@Ag nanobars in which gold NRs are in the corner positions of the nanobars and their longitudinal axes parallel the longer sides of the nanobars. In this work, the position of Au NRs in the corner of Au@Ag nanobars is quite different from that in the center reported by the previous literature [10, 11]. These peculiar Au@Ag nanobars could be useful as catalysts [20] and substrate surfaces in enhanced nonlinear optics [21].

Acknowledgments The authors gratefully acknowledge Dr. Joseph Kuo-Hsiang Tang at Clark University (Worcester, MA, USA) for numerous insightful discussions. This work was supported by a Grant from the National Science Council of Taiwan (NSC 99-2113-M-032-001).

References

1. N.R. Jana, L. Gearheart, C.J. Murphy, J. Phys. Chem. B **105**, 4065 (2001)
2. B. Nikoobakht, M.A. El-Sayed, Chem. Mater. **15**, 1957 (2003)
3. R.C. Wadams, L. Fabris, R.A. Vaia, K. Park, Chem. Mater. **25**, 4772 (2013)
4. L. Scarabelli, M. Grzelczak, L.M. Liz-Marzán, Chem. Mater. **25**, 4232 (2013)
5. M.W. Chu, V. Myroshnychenko, C.C. Chen, J.P. Deng, C.Y. Mou, F.J. García de Abajo, Nano Lett. **9**, 399 (2009)
6. E. Carbó-Argiby, B. Rodríguez-González, J. Pacifico, I. Pastoriza-Santos, J. Pérez-Juste, L.M. Liz-Marzán, Angew. Chem. Int. Eng. **46**, 8983 (2007)
7. W. Ni, X. Kou, Z. Yang, J. Wang, ACS Nano **2**, 677 (2008)
8. K. Sohn, F. Kim, K.C. Pradel, J. Wu, Y. Peng, F. Zhou, J. Huang, ACS Nano **3**, 2191 (2009)
9. Y. Okuno, K. Nishioka, N. Nakashima, Y. Niidome, Chem. Lett. **38**, 60 (2009)
10. Y. Okuno, K. Nishioka, A. Kiya, N. Nakashima, A. Ishibashi, Y. Niidome, Nanoscale **2**, 1489 (2010)
11. K. Park, L.F. Drummy, R.A. Vaia, J. Mater. Chem. **21**, 15608 (2011)
12. J. Zeng, Y. Zheng, M. Rycenga, J. Tao, Z. Li, Q. Zhang, Y. Zhu, Y. Xia, J. Am. Chem. Soc. **132**, 8552 (2010)
13. J. Becker, I. Zins, A. Jakab, Y. Khalavka, O. Schubert, C. Sönnichsen, Nano Lett. **8**, 1719 (2008)
14. K.J. Tu, S.Y. Chen, J.P. Deng, J. Chin. Chem. Soc. **57**, 950 (2010)
15. P.K. Sudeep, S.T. Shibu Joseph, K.G. Thomas, J. Am. Chem. Soc. **127**, 6516 (2005)
16. K.G. Thomas, S. Barazzouk, B. Ipe, S.T. Shibu Joseph, P.V. Kamat, J. Phys. Chem. B **108**, 13066 (2004)
17. C.J. Murphy, T.K. Sau, A.M. Gole, C.J. Orendorff, J. Gao, L. Gou, S.E. Hunyadi, T. Li, J. Phys. Chem. B **109**, 13857 (2005)
18. X. Kou, S. Zhang, Z. Yang, C. Tsung, G.D. Stucky, L. Sun, J. Wang, C. Yan, J. Am. Chem. Soc. **129**, 6402 (2007)
19. S. Gómez-Graña, B. Goris, T. Altantzis, C. Fernández-López, E. Carbó-Argibay, A. Guerrero-Martínez, N. Almora-Barrios, N. López, I. Pastoriza-Santos, J. Pérez-Juste, S. Bals, G.V. Tendeloo, L.M. Liz-Marzán, J. Phys. Chem. Lett. **4**, 2209 (2013)
20. W. Wang, J. Zhang, F. Chen, Res. Chem. Intermed. **36**, 163 (2010)
21. J. Gu, Y. Li, W. Li, J. Shi, Res. Chem. Intermed. **35**, 807 (2009)